Histol Histopathol (2010) 25: 1581-1590

http://www.hh.um.es

Histology and Histopathology

Cellular and Molecular Biology

Cardiovascular autonomic neuropathy in spontaneously diabetic rats with and without application of EGb 761

Rick Schneider[1], Klaus Welt[2], Wolfram Aust[3], Regina Kluge[4], Heinz Löster[5] and Günther Fitzl[2]

[1]Department of Surgery II, [2]Institute of Anatomy, [3]Department of Otorhinolaryngology, [4]Department of Nucler Medicine, and [5]Institute of Laboratory Medicine, Clinical Chemistry and Molecular Diagnostics, University of Leipzig, Leipzig, Germany

Summary. Cardiovascular autonomic neuropathy causes abnormalities in the diabetic heart with various clinical sequelae, including exercise intolerance, arrhythmias and painless myocardial infarction. Little is known about (ultra)structural alterations of the myocardial nervous network. On the assumption that this diabetes-specific neuropathy develops due to permanently increased oxidative stress by liberation of oxygen-free radicals, adjuvant application of antioxidative therapeutics appears promising in preventing or delaying long-term diabetic complications. We have investigated the effects of Ginkgo biloba extract (EGb 761), a radical scavenger, against diabetes-induced myocardial nervous damage in spontaneously diabetic BioBreeding/Ottawa Karlsburg (BB/OK) rats. Morphological and morphometric parameters were evaluated by electron microscopy. We used immunohistochemistry to investigate protein expression of protein gene product 9.5, S100 protein, and thyroxin hydroxylase as a neuronal marker. Alterations of cardiac sympathetic activity were measured using the in vivo ^{123}I-metaiodobenzyl-guanidine imaging, and the immunofluorescent labeling of beta1-adrenergic receptors and adenylate cyclase. Our results revealed that A) Diabetes results in slight to moderate ultrastructural alterations (hydrops, disintegration of substructure) of autonomic nerve fibers and related Schwann cells in untreated BB diabetic rats; B) Cardiac sympathetic integrity and activity is impaired due to alterations in the presynaptic nerve terminals and the postsynaptic $ß_1$-AR-AC coupling system; C) Pre-treatment of diabetic myocardium with EGb results in an improvement of most of these parameters compared to unprotected myocardium. In conclusion, EGb may act as a potent therapeutic adjuvant in diabetics with respect to cardiovascular autonomic neuropathy, which may contribute to the prevention of late complications in diabetes.

Offprint requests to: Rick Schneider, Department of Surgery II, University of Leipzig, Liebigstr. 20, Leipzig, 04103, Germany. e-mail: rick.schneider@medizin.uni-leipzig.de

Key words: Diabetes, Cardiovascular autonomic neuropathy, ^{123}I-MIBG imaging, Egb 761, Oxidative stress

Introduction

The cardiovascular autonomic neuropathy (CAN) is one of the most overlooked of all serious complications of diabetes, and is associated with the development of diabetic cardiomyopathy with subsequent increased mortality because of silent ischemia and myocardial infarction (Maser and Lenhard, 2005; Vinik and Ziegler, 2007). Hyperglycemia and hyperlipidemia may result in several major cellular metabolic perturbations. Formation of advanced glycation end products (AGEs) and reactive oxygen species (ROSs) lead to structural alterations of diabetic cardiomyocytes, microvasculature and interstitium, as previously shown in spontaneously diabetic BioBreeding/OttawaKarlsburg (BB) rats (Schneider et al., 2008, 2009).

Although neuropathologic changes are not completely understood, both the sympathetic and parasympathetic nervous system might be involved in CAN (Sharma and McNeill, 2006; De Angelis et al., 2009). A progressive loss and severe structural abnormalities of sympathetic nerve fibres, as well as alterations of cardiac cell surface beta-adrenoceptors, has been described in the myocardium of spontaneously and STZ-diabetic rats (Atkins et al., 1985; Yagihashi and Sima, 1985; Rösen et al., 1995). As a result of damage of the autonomic nerves, the interplay of sympathetic and parasympathetic activity is disturbed (Debono and Cachia, 2007). However, it is well known that ventricular tissue is innervated mainly by sympathetic nerves, whereas parasympathetic fibres are much less numerous (Cao et al., 2000). Most cardiac nerves have a sheath of Schwann, like other peripheral nerves (Chen et

al., 2001). Immunohistochemical techniques allow specific staining of Schwann cells using S100 protein (S100) antibody, cardiac nerves using protein gene product 9.5 (PGP9.5) antibody, and sympathetic nerves using the tyrosine hydroxylase (TH) antibody, besides many others.

A direct, noninvasive in vivo approach for the assessment of cardiac sympathetic activation is the use of ^{123}I-Metaiodobenzylguanidine (MIBG). MIBG is a compound with affinity for the neuronal noradrenaline uptake mechanisms, and it is not subjected to monoamine oxidase or catechol-o-methyltransferase enzymatic catabolism. The level of neuronal uptake of MIBG is assumed to reflect the neuronal integrity of the sympathetic system of the heart, whereas the wash-out rate should be proportional to sympathetic activity (Scott and Kench, 2003; Kusmic et al., 2008).

Assuming that diabetic damage is partly caused by increased oxidative stress by the occurrence of oxygen-free radicals, and some late complications in chronic diabetes cannot be completely avoided by insulin therapy (Addicks et al., 1993), the application of radical scavengers seems promising as shown by Rösen et al. (1995).

The aim of this study was to characterize (ultra)structural alterations in cardiac nerve fibres and related Schwann cells of BB diabetic rats as a model of human diabetes type I, to visualize the cardiac nerve fibres and Schwann cells by different immunohistochemical techniques, and to get further insight into sympathetic neuronal integrity and activity by immunofluorescent technique and the in vivo approach using MIBG imaging. Pretreatment with Ginkgo biloba extract (EGb761) is used to show whether protection of the autonomic nerves is possible.

Materials and methods

Animals and experimental procedure

The experiments were approved by Leipzig's regional governing committee (Regierungspraesidium No. 10/00) and have been performed in accordance with local animal welfare legislation. 17 male diabetic BioBreeding/Ottawa Karlsburg (BB/OK) rats aged eight to nine months and ten male non-diabetic BB/OK rats of the same age (http://www.medizin.uni-greifswald.de/labanim/available_rat. html) kept separately under semisterile conditions were divided into three experimental groups.

The non-diabetic BB/OK animals were not subjected to any treatment. The diabetic BB/OK rats manifested insulin-dependent diabetes after 106±28.3 days as identified by weekly measurement of blood glucose levels. When plasma glucose levels exceeded 23.8 mmol/l, the rats were treated by subcutaneous sustained-release insulin implant (LINDPLANT. LINSHIN Canada, INC., Scarborough, Ontario, Canada). The diabetic BB/OK rats were divided into two groups: 10 animals were sacrificed after six months of diabetes; 7 rats were treated with Ginkgo biloba extract (EGb, IPSEN Paris, France) after three months of diabetes, and were sacrificed after six months of diabetes including three months of protection by EGb. EGb treatment was provided daily with 100 mg/kg body weight of Ginkgo biloba extract dissolved in a limited amount of drinking water and administered overnight.

^{123}I-MIBG imaging

Two weeks before sacrifice, five rats of each group were anesthetized using ketamin (100mg/kg, intraperitoneally), and received 4MBq ^{123}I-MIBG (Amersham Buchler) intravenously into a tail vein. Whole rat dynamic planar imaging studies were then performed, during 1 h, on a digicam-camera MB 9000-300 (equipped with a pin-hole collimator; Budapest, Hungary). Subsequently, static images were acquired every 30 min from 1 to 4 h p.i. Regions of interest were drawn manually around the heart and average counts per pixel were measured. Values were corrected for matrix size, injected dose (in μCi), decay and body weight and thus expressed as average counts x kg body weight/pixel x I.D.

Tissue processing for light microscopy

The animals were anesthetized using pentobarbital. The heart was rapidly excised after thoracotomy, and tissue samples from all groups were taken from the left ventricle near the apex by scalpel and processed for histology, electron microscopy, and immunohistochemistry as described below.

Tissue processing for electron microscopy

Tissue samples were minced into small blocks of about 1 mm^3, fixed in cold Karnovsky's solution (buffered 2% glutardialdehyde, 2% paraformaldehyde, pH 7.4) for two hours, contrasted with OsO_4 and phosphotungstic acid, and embedded in Durcupan (FLUKA) after acetone dehydration.

Semithin sections from each block were stained with toluidine blue to select areas of interest for electron microscopy. Ultrathin sections were obtained using Ultracut E (Reichert-Jung) and contrasted with uranyl acetate and lead citrate solution. Electron micrographs according to the requirements of morphometry were taken using an EM 900 (Zeiss).

Semiquantitative analysis of ultrastructure

For semiquantitative evaluation of ultrastructure we analyzed one hundred electron micrographs per animal per group (1,000 micrographs of non-diabetic BB rats, 1,000 micrographs of untreated diabetic BB rats, and 700 micrographs of the EGb-treated diabetic BB rats) at 12,000-fold primary magnification obtained from five

tissue blocks. All samples were blinded to the experimental groups. Axonal edema, swelling, rarefication, or degeneration of mitochodria, and/or structural loss of axonal filaments were defined as injury characteristics of autonomic nerves. Cellular edema, swelling, rarefication, or degeneration of mitochondria, and/or alterations of basal membrane of Schwann cells were defined as injury characteristics of Schwann cells. The percentages of altered axons vs. Schwann cells were semiquantitatively evaluated.

Immunohistochemical techniques

Five serial sections per animal were deparaffinized, rehydrated in a descending alcohol cascade, treated using 3% H_2O_2 solution, rinsed in distilled water, treated in TBS (Tris buffer saline) and stored in serum protein block (DAKO). Sections were stored overnight with the primary antibody at different dilutions ranging from 500 to 2,000:1 at 4°C in a moist chamber. After that, they were rinsed in TBS, stored for one hour with the diluted secondary antibody at room temperature, rinsed again in TBS, stored with PAP (peroxidase-antiperoxidase) complex (rabbit or mouse EnVision, DAKO) diluted in Tris buffer or avidin-biotinylated enzyme complex (Vectastain ABC Kit, VACTOR LABORATORIES), and rinsed three times in TBS. After reaction with the DAB set, the sections were developed for 1-5 min, rinsed in distilled water, dehydrated in an ascending alcohol cascade, and embedded in Canada balsam.

Primary antibodies. Rabbit polyclonal PGP9.5 (Biotrend); Rabbit polyclonal S100 (Immunotech); Rabbit polyclonal TH (Biotrend).

Secondary antibodies. Goat anti-rabbit IgG (Vektor Laboratories)

Controls for immunostaining of PGP9.5, S100 and TH. Negative controls: incubation a: without primary antibody; b: without secondary antibody. Positive controls: incubation of known positive tissue (rat small bowel and brain).

Immunofluorescence

Five serial cryostat sections per animal were fixed with acetone. After blocking of non-specific binding sites in serum protein block, serum-free (DAKO), the cryostat sections were stained using standard immunofluorescent protocols. The sections were incubated overnight at 4°C in a moist chamber with primary antibodies at dilution 1:20: polyclonal anti-rabbit beta1-adrenergic receptor ($ß_1$-AR) (Santa Cruz), polyclonal anti-rabbit adenylate cyclase (AC) (Santa Cruz), rinsed in TBS. The specificity of antibodies was controlled by omitting of primary antibodies. Detection of bound primary antibodies was performed with goat anti-rabbit conjugated FITC (Santa Cruz) at a dilution 1:100. Labeled samples were mounted with ProTexMountFluor (quartett), and examined under a BX-FLA reflected light fluorescence microscope (OLYMPUS) equipped with appropriate filters.

Semiquantitative evaluation of immunohistochemical and immunofluorescent staining

A semiquantitative evaluation of the extent and intensity of PGP9.5, S100, TH, $ß_1$-AR, and AC reaction was independently conducted by three observers. Fifty microscopic fields of view (FOV) per animal per group (500 FOV of non-diabetic BB rats, 500 FOV of untreated diabetic BB rats, and 350 FOV of the EGb-treated diabetic BB rats) were analyzed. All samples were blinded to the experimental groups. The scoring method used in this evaluation was adapted from Bishop et al. (2004), and included four grades as follows: Grade 1, focal and minimal staining intensity; Grade 2, focal and medium staining intensity; Grade 3, covered area and medium staining intensity; Grade 4, covered area and most intensive staining. After each observer analyzed the microscopic FOV for degree of extent and intensity of PGP9.5, S100, TH, $ß_1$-AR, and AC reaction, the mean of the individual observations was calculated.

Statistics

Data for myocardial morphometric analyses and 123I-MIBG imaging are expressed as the means ± SD. Statistical differences between mean values were calculated using Student's t-test for unpaired values, and were considered significant at values of $p<0.05$; Wilcoxon's test was used for non-parametric variables. The SPSS+ software package was used for each statistical evaluation.

Results

Qualitative and quantitative electron microscopic findings

The ultrastructural pattern of autonomic nerves of diabetic myocardium was characterized by the coexistence of components that were either apparently normal or damaged to a greater or lesser degree. Scattered areas of unmyelinated axons showed dystrophic and degenerative changes. Axoplasmic lysis was frequent in dystrophic axons while many of the remaining axons had clod-like segregated cytoplasm with mal-orientated neurofilaments, and moderate swelling of mitochondria, which showed varying degrees of matrix clearing and partial disintegration of internal membranes. Other axons showed degenerated mitochondria, accumulations of dense bodies and organelle debris.

Schwann cells were progressively altered, showing enlarged mitochondria partly accompanied by disintegration of membranes and/or disarrangement of cristae, and proliferated and thickened basal laminae with collagen pockets. An increased amount of organelle debris as well as bundles of small fibres in the dilated interstitium and around Schwann cells was noticeable in

the unprotected diabetic group.

Semiquantitative analysis of unmyelinated nerves and related Schwann cells in unprotected diabetic myocardium revealed ultrastructural alterations in comparison with healthy controls. The percentages of both altered autonomic nerves and related Schwann cells

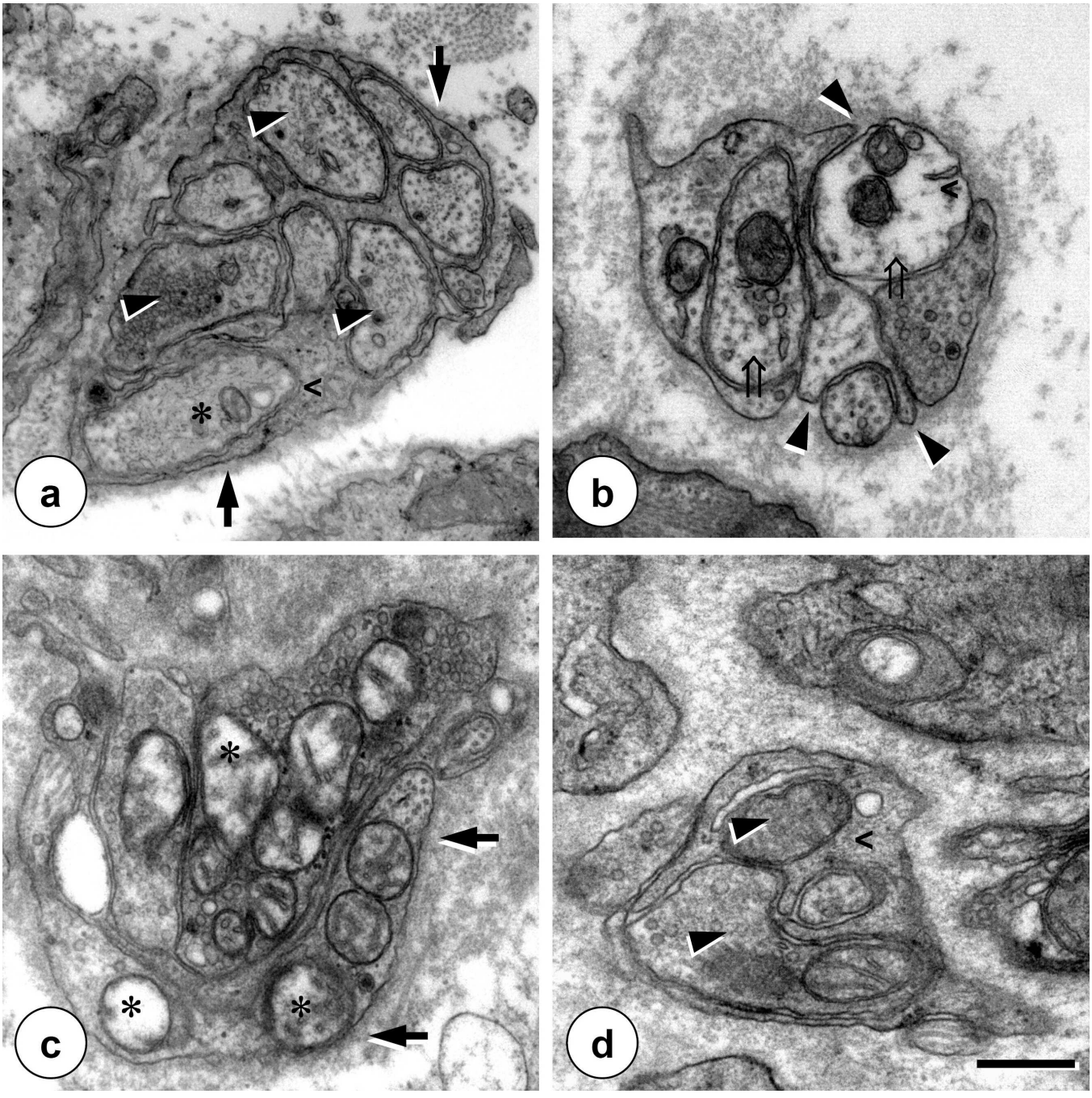

Fig. 1. Autonomic nerve fibres and related Schwann cells in the myocardium of the experimental groups. **a.** Normal ultrastructure of autonomic nerve in non-diabetic control animals with normal aspect of axons [arrowhead] and related Schwann cell [left chevron], normal mitochondria [asterisk] and normal thickness of basal lamina [arrow]. **b and c.** Autonomic nerve from an untreated ischemic rat showing axoplasmic lysis with loss of neurofilaments [empty arrow] and organelle debris [left chevron]. Mitochondria [asterisk] are partly damaged (swelling, clearing of the matrix, cristolysis with disintegration of internal membranes). Schwann cell of an untreated diabetic rat showing markedly thickened basal lamina [arrow] and partial disintegration of axons [arrowhead]. **d.** EGb-protected autonomic nerve from a diabetic rat exhibiting nearly normal ultrastructure (axons [arrowhead], related Schwann cell [left chevron]). Scale bar: 2.0 μm.

were increased in diabetic myocardium. In contrast, the ultrastructure of autonomic nerves and Schwann cells of the EGb-protected diabetic myocardium appeared significantly less altered than in unprotected diabetic animals. Irregularities of axonal texture, partial loss of neurofilaments, mitochondrial swelling, and internal disintegrations, as well as structural alterations of Schwann cells, appeared less expressed (Fig. 1). A slight dilatation caused by edema was regionally evident. EGb treatment led to significant improvement of the semiquantitative ultrastructural parameters (Table 1).

Immunohistochemical demonstration of PGP9.5, S100, and TH expression

Nerve fibre immunoreactivities to PGP9.5, S100 and TH were easily observed between the myocytes and along blood vessels. All experimental groups showed an inhomogeneous distribution of the reaction product, either as fibre-associated chain-like varicosities closely related to the longitudinal axis of cardiomyocytes, or as isolated perivascular nerve trunk or fascicle-like structures. The staining intensities of PGP9.5, S100 and TH were strong in control rats, but reduced in untreated diabetes. The distribution of nerves was much less homogenous in untreated diabetic myocardium. EGb treated animals showed a protein expression near to control levels (Fig. 2). Table 2 showed the results of the immunohistochemical grading for PGP9.5, S100 and TH in all groups.

Immunofluorescent demonstration of $ß_1$-AR and AC

With immunofluorescence technique, $ß_1$-AR were found on the surface of cardiomyocytes from all experimental groups showing an inhomogeneous, dot-like pattern with and without striation. Especially around larger vessels, there were clusters with higher intensity. In all preparations there was no, or less, immunofluorescence in the intercellular space. However fluorescence was seen in endothelial cells of venules and capillaries. Immunofluorescence was strong in myocardium of control animals, but weak in untreated diabetes. EGb treated diabetic animals showed a more intense fluorescence near to control levels (Fig. 3).

In general, a striated pattern of AC was found on the inner surface of cardiomyocytes from all experimental groups with only slight differences in semiquantitative evaluation. Fluorescence was ubiquitous in all preparations. However there was no, or less, immunofluorescence in the intercellular space. Immunofluorescence of AC was strong in cardiomyocytes from control rats, but reduced in untreated diabetes. EGb treatment led to a more intense fluorescence near to control levels.

Table 3 summarizes the results of the immunofluorescent grading for $ß_1$-AR and AC of all groups.

Table 1. Semiquantitative evaluation of ultrastructural pattern of autonomic nerves and related Schwann cells in the in experimental groups (left ventricle).

	Control		Diabetes		Diabetes+EGb 761
Percentage of altered autonomic nerves	5.8±4	*	20.5±7	*	11.3±7
Percentage of altered Schwann cells	8.1±5	*	33.3±9	*	19.4±8

Criteria for alterations defined as axonal edema, swelling, rarefication, or degeneration of mitochodria, and/or structural loss of axonal filaments for autonomic nerves; and cellular edema, swelling, rarefication, or degeneration of mitochodria, and/or alterations of basal membrane of related Schwann cells (mean ± SD) (*p≤ 0.05).

Table 2. Semiquantitative evaluation of immunohistochemical stained protein gene product 9.5 (PGP9.5), S100 protein (S100), and tyrosine hydroxylase (TH) (left ventricle) in experimental groups (mean ± SD) (*p≤0.05).

	Control		Diabetes		Diabetes+EGb 761
PGP9.5	2.7±0.1	*	1.4±0.2	*	2.4±0.3
S100	2.0±0.1	*	1.2±0.1	*	2.3±0.2
TH	2.5±0.2	*	1.9±0.2		2.4±0.1

Table 3. Semiquantitative evaluation of immunofluorescent presentation of beta$_1$-adrenergic receptors ($ß_1$-AR) and adenylate cyclase (AC) (left ventricle) in experimental groups (mean ± SD) (*p≤0.05).

	Control		Diabetes		Diabetes+EGb 761
$ß_1$-AR	2.7±0.3	*	1.5±0.1	*	2.3±0.1
AC	2.8±0.5	*	1.9±0.1		2.5±0.6

Table 4. ^{123}I-MIBG imaging in anesthetized BB/OK rats from all experimental groups 1 and 4 h after the intravenous administration of 4MBq ^{123}I-MIBG.

	Control		Diabetes		Diabetes+EGb 761
uptake	7.8±0.8	*	4.6±1.5		5.4±2.1
washout	36.1 ± 6.7		27.8 ± 5.7	*	37.9 ± 2.3

Uptake of ^{123}I-MIBG: average counts x kg body weight / pixel x injected dose; washout rate: %; (mean ± SD) (*p≤0.05).

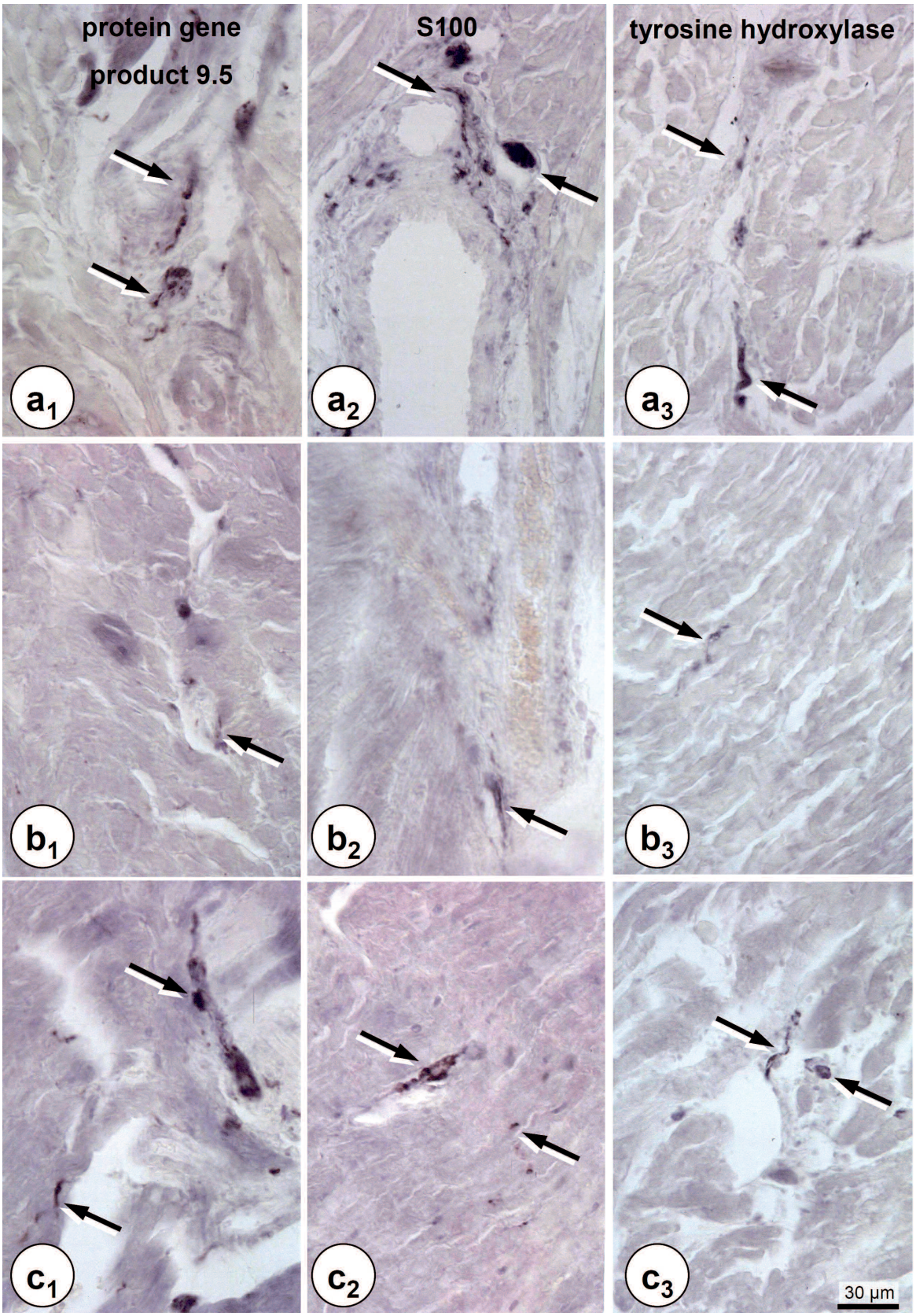

Fig. 2. Immunohistochemical localization of S100, and specific nerve markers protein gene product 9.5 (PGP9.5) and tyrosine hydroxylase (TH) in myocardium from all experimental groups showing an inhomogeneous distribution of the reaction product, either as fibre-associated chain-like varicosities closely related to the longitudinal axis of cardiomyocytes or as isolated perivascular nerve trunk or fascicle-like structures. **a.** Control rats: normal appearance with strong immunostaining for S100, PGP9.5 and TH (arrow). **b.** Diabetic rats: weaker immunostaining for S100, PGP9.5 and TH (arrow). **c.** EGb-protected diabetic rats: stronger immunostaining for S100, PGP9.5 and TH (arrow).

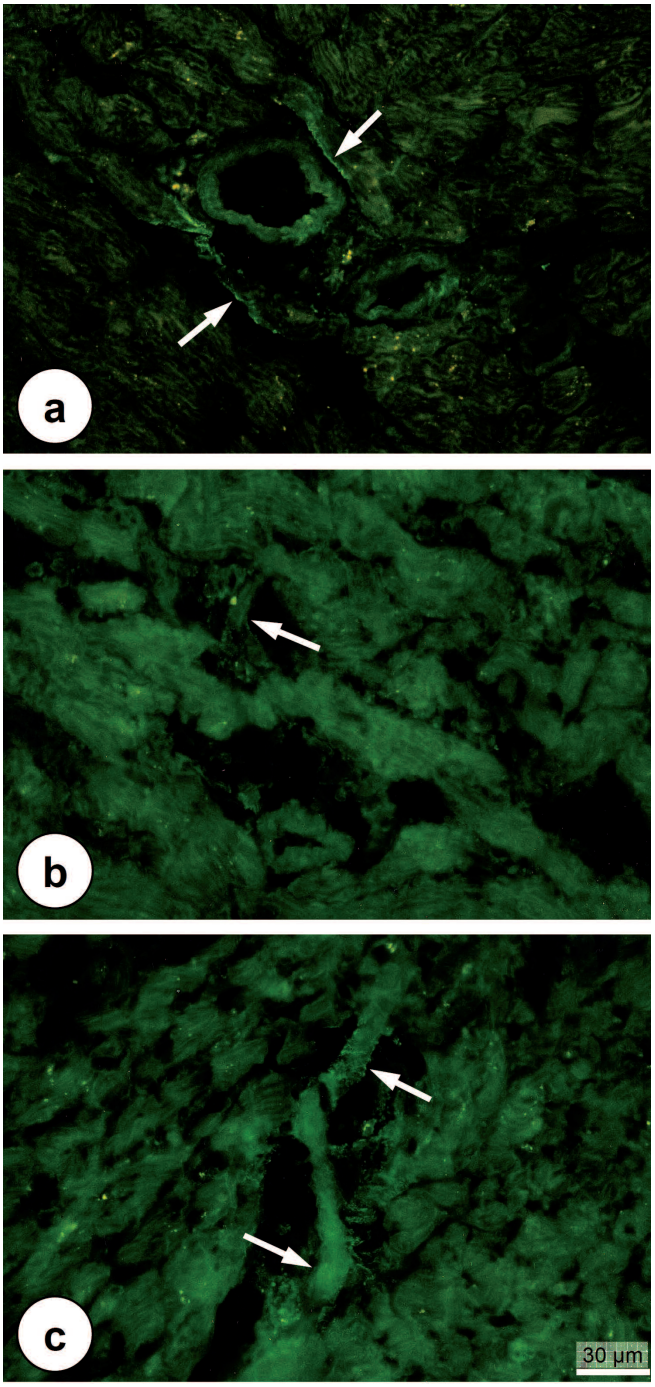

Fig. 3. Immunofluorescent demonstration of ß1-adrenergic receptors in myocardium showing an inhomogeneous dot-like pattern with clusters of higher intensity mainly around larger vessels in cardiomyocytes from all experimental groups. **a.** Control rats: strong immunofluorescence of ß1-adrenergic receptors (arrow). **b.** Diabetic rats: weaker immunofluorescence of ß1-adrenergic receptors (arrow). **c.** EGb-protected diabetic rats: stronger immunofluorescence of ß1-adrenergic receptors (arrow).

^{123}I-MIBG imaging

The evaluation of the MIBG scintigraphic parameters showed a significant lower level of uptake rate in the heart 1h after injection in the untreated diabetic rats when compared to the non-diabetic rats. Wash-out rates were lower in the untreated diabetic rats than in the healthy control animals. However, this difference was not statistically significant.

In the EGb treated rats values of MIBG uptake and wash-out rate were near to control levels (Fig. 4).
Table 4 shows the results of MIBG imaging in all groups.

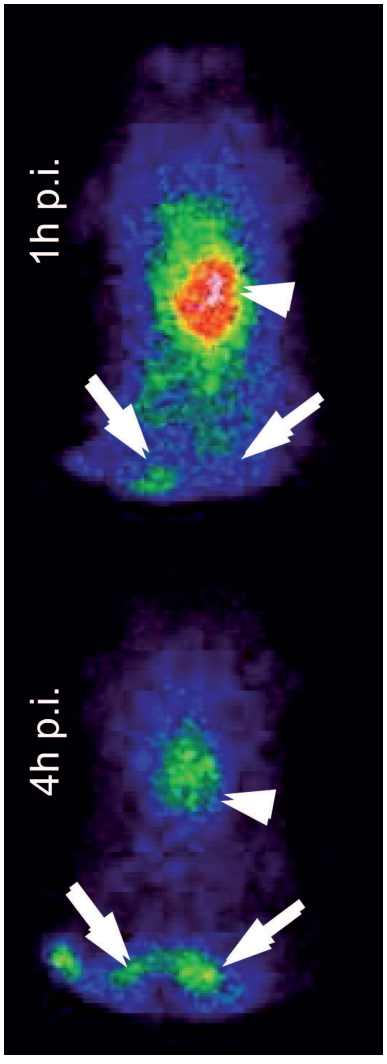

Fig. 4. Whole-body scintigrams of an anesthetized untreated diabetic BB/OK rat 1 and 4 h after the intravenous administration of 4MBq ^{123}I-MIBG, performed on a digicam-camera MB 9000-300, equipped with a pin-hole collimator. The heart as the region of interest [arrowhead], renal clearance of ^{123}I-MIBG (kidneys [arrow]).

Discussion

As described by Yagihashi and Sima (1985), the spontaneously diabetic BB rats appear to be a suitable animal model for the study of functional and structural abnormalities and the pathogenesis of diabetic neuropathic complications. Our findings of cardiac nerve fibres and related Schwann cells indicate a structural loss of autonomic predominant sympathetic fibres, as well as Schwann cells, in untreated diabetic hearts as also shown in the literature (Rösen et al., 1995; Jeon et al., 2000). This genuine neuronal loss may impair the complex network of cardiac nerves, comprising both putative sensory and widely distributed autonomic components (Chen et al., 2001). In contrast, Park et al. (2002) found increased sympathetic nerve regeneration with an increase in nerve sprouts and overactivity in the myocardium.

The observed axonal dystrophic changes of autonomic nerves have also been reported from other authors as the main pathological features of CAN in rats with spontaneous and streptozotocin-induced diabetes (Addicks et al., 1993; Yagihashi, 1995; Schmidt et al., 1997). Qualitative changes of Schwann cells appeared milder, as described by others (Yagihashi and Sima, 1985; Rösen et al., 1995). These morphological alterations may represent the structural correlate for a slowly progressive axonopathy with a decrease in orthograde and/or retrograde axoplasmic transport leading up to axonal atrophy, as demonstrated in different autonomic and somatic C-fibres in BB diabetic rats (Yagihashi and Sima, 1986; Yagihashi et al., 1989). Swelling or increase in number of organelles, mal-orientated neurofilaments, disturbed mechanisms for removal of intraaxonal organelles, and/or simply edema must be discussed as reasons for dilated axons in diabetes. Mitochondrial accumulation may reflect alterations in axonal transport, and produce an abnormal subcellular environment. The hyperglycemia-induced process of overproduction of superoxide by the mitochondrial electron-transport chain results in the development of neuronal toxicity (Brownlee, 2001; Schmidt et al., 2003). Furthermore, the nerve loss caused by glucose-induced apoptosis, overproduction of tumor necrosis factor alpha and other cytokines, endoneurial ischemia as a result of microvascular alterations, and downregulation of the potent chemoattractants, nerve growth factor and nerve insulin-like growth factor-1, with impaired nerve fibre regeneration, may also be involved in the pathogenesis of diabetic cardiac neuropathy (Vinik et al., 2003; Ieda and Fukuda, 2009).

It is shown that diabetes alters the density, sensitivity, and responsiveness for ß-AR with impairment of the coupled AC in the heart. However, the effects of diabetes on ß-AR expression and downstream signalling are controversial (Dinçer et al., 2001; Sharma et al., 2008). Mainly in the early stage of diabetes, an activation of the sympathetic nervous system contributes to myocardial damage with increased apoptosis and necrosis, predominantly by stimulation of $ß_1$-AR (Lohse et al., 2003; Zhu et al. 2003; Sharma and McNeill, 2006). In accordance with diminished functional response (Dinçer et al., 2001), we can demonstrate a decrease in $ß_1$-AR density on cardiac membranes in untreated chronic diabetic rats, as has also been shown in STZ-diabetic myocardium by Atkins et al. (1985). Elevated noradrenaline levels may result in agonist-induced desensitization and downregulation, as well as decreased synthesis of $ß_1$-AR (Carrió, 2001; Camici, 2002). It appears more probable that ARs undergo internalisation and degradation affected by nonenzymatic glucosylation, or that other glucosylated peptides interfere with normal receptor function, producing subsequent alterations in the ligand binding characteristics, in the position of the receptor in the membrane lipid milieu, or in the catabolism of ARs (Atkins et al., 1985). A reduction of $ß_1$-AR mRNA and protein levels may indicate an impairment of receptor synthesis at the level of transcriptional regulation (Altan et al. 2007). In accordance with the findings of Sethi et al. (2003), we found a diminished AC protein expression in untreated diabetic myocardium. Pathological steps in the transmembrane signalling, mainly caused by oxidative stress with desensitization of AC, may result in uncoupling of $ß_1$-AR-AC complex (Gando et al., 1993). It is controversial, whether the coupling protein rather than AC itself is more affected by oxidative stress. Although AC is the target of free radicals, the irreversible inactivation may actually be mediated by a reduction of membrane fluidity by lipid peroxidation in diabetes (Haenen et al., 1990).

Quantitative MIBG imaging allows assessment of myocardial sympathetic integrity and activity in diabetes (Scott and Kench, 2004). In contrast to the non-neuronal uptake-2 mechanism, the uptake-1 mechanism predominates in cardiac MIBG imaging because of the small quantity of injection (Verberne et al., 2008). In accordance with the findings of Camacho and Carrió (2007), our profound loss of myocardial uptake reflects neuronal dysfunction in direct correlation to our ultrastructural and immunohistochemical results, suggesting a structural impairment as well as an absolute loss of sympathetic nervous tissue. In contrast to the literature (Kim et al., 1996; Standl and Schnell, 2000), we found a decrease in myocardial MIBG washout rate in the untreated diabetic group, suggesting a diminished adrenergic activity. Because of the reported increased sympathetic activity associated with high myocardial MIBG washout at the early stage of diabetes, we presume that the impaired nervous integrity with substantial loss of fibres, as well as alterations of the $ß_1$-AR-AC coupling system, may result in an absolute loss of neurotransmitters with subsequent diminished sympathetic activity in chronic diabetes. These changes may reflect a decrease of catecholamine production in the myocardium (Togane, 1999). Furthermore, the reduction in neuronal reuptake of norepinephrine, rather than the loss of neuronal endings, has been suggested to explain the acceleration in the observed myocardial tracer washout (Kusmic et al., 2008). Intraneuronal

ischemia in diabetes would be expected to decrease the efficiency of the vesicular monoamine transporter or cell membrane norepinephrine transporter, activities which depend on energy-requiring processes (Goldstein, 2003; Kiyono et al., 2005).

It appears logical to apply adjuvant therapies to scavenge oxygen free radicals that occur during diabetic metabolism and lead to generation of AGEs. In our case, the combined activities of the constituents of EGb (24% flavonoids, 6% terpenoids, 8% ginkgolides) are responsible for the therapeutic benefit observed, as seen by others with vitamin E treatment (Rösen et al., 1995). The lipophilic property of the main components explains the high affinity to biological membranes.

The protective effects of Ginkgolide A may be attributed to the inhibition of protein kinase C (Bäcklund et al., 2004), as well as the direct antioxidative and free radical-quenching potential of EGb, which evidently result in reduced formation of AGEs and improvement of the antioxidative capacity of myocardium (Pietri et al., 1997). EGb might attenuate the rarefication in the neuronal network of diabetic myocardium, as described in STZ-diabetes by Zhang et al. (2005). The terpenoid constituents and flavonoid metabolites probably act in a complementary manner to protect against diabetes-induced alterations (Liebgott et al., 2000), such as intracellular acidification and cellular protease activation, resulting in protein degradation (Giraldez et al., 1997), or specific fragmentation and inactivation (Taniguchi et al., 1989). Improvement in hemodynamic features and transport of vasoactive substances promote neuronal function. Bilobalides stabilize mitochondrial function and ATP synthesis, and improve the osmotic milieu. The direct membrane-stabilizing and anti-edematous potential of EGb (Huang et al., 1981) may lead to endoneuronal permeability regulation with decreased protein extravasation and interstitial edema, resulting in stabilization of the presynaptic integrity and postsynaptic $ß_1$-AR-AC coupling system.

In this respect, we presume that EGb may improve the above-mentioned parameters. Radioiodinated MIBG is a relieable marker for the detection of cardiac neuronal damage in BB spontaneous diabetic CAN.

In conclusion, the independent evaluation of ultrastructural, immunohistochemical, and immuno-fluorescent parameters, as well as in vivo radioactive investigations, show convincingly the impairment of autonomic, predominantly sympathetic, innervation of diabetic myocardium of untreated BB rats, and the protective effect of EGb substitution.

Acknowledgements. We are very grateful to the IPSEN Institute, Paris, for providing us with the EGb. We wish to thank Prof. Dr. Klöting (Department of Laboratory Animal Science, Medical Faculty, University of Greifswald, Karlsburg, 17495, Germany) for providing the BB/OK rats, and the animal breeding centre of the medical faculty of the University of Leipzig, especially Dr. Madaj-Sterba and Mrs. Weisheit, for their careful therapeutic management of the animals. We would like to thank Mrs. Craaz, Mrs. Schneider and Mrs. Brachmann for their excellent technical assistance.

References

Addicks K., Boy C. and Rösen P. (1993). Sympathetic autonomic neuropathy in the heart of the spontaneous diabetic BB rat. Anat. Anz. 175, 253-257.

Altan V.M., Arioglu E., Guner S. and Ozcelikay A.T. (2007). The influence of diabetes on cardiac beta-adrenoceptor subtypes. Heart Fail. Rev. 12, 58-65.

Atkins F.L., Dowell R.T. and Love S. (1985). Beta-Adrenergic receptors, adenylate cyclase activity, and cardiac dysfunction in the diabetic rat. J. Cardiovasc. Pharmacol. 7, 66-70.

Bäcklund T., Palojoki E., Saraste A., Eriksson A., Finckenberg P., Kytö V., Lakkisto P., Mervaala E., Voipio-Pulkki L.M., Laine M. and Tikkanen I. (2004). Sustained cardiomyocyte apoptosis and left ventricular remodelling after myocardial infarction in experimental diabetes. Diabetologia 47, 325-330.

Bishop J.B., Tani Y., Witt K., Johnson J.A., Peddada S., Dunnick J. and Nyska A. (2004). Mitochondrial damage revealed by morphometric and semiquantitative analysis of mouse pup cardiomyocytes following in utero and postnatal exposure to zidovudine and lamivudine. Toxicol. Sci. 81, 512-517.

Brownlee M. (2001). Biochemistry and molecular cell biology of diabetic complications. Nature 414, 813-820.

Camacho V. and Carrió I. (2007). Targeting neuronal dysfunction and receptor imaging. Curr. Opin. Biotechnol. 18, 60-64.

Camici P.G. (2002). Imaging of cardiac adrenergic innervation. Heart 88, 209-210.

Cao J.M., Fishbein M.C., Han J.B., Lai W.W., Lai A.C., Wu T.J., Czer L., Wolf P.L., Denton T.A. and Shintaku I.P. (2000). Relationship between regional cardiac hyperinnervation and ventricular arrhythmia. Circulation 101, 1960-1969.

Carrió I. (2001). Cardiac neurotransmission imaging. J. Nucl. Med. 42, 1062-1076.

Chen P.S., Chen L.S., Cao J.M., Sharifi B., Karagueuzian H.S. and Fishbein M.C. (2001). Sympathetic nerve sprouting, electrical remodeling and the mechanisms of sudden cardiac death. Cardiovasc. Res. 50, 409-416.

De Angelis K., Irigoyen M.C. and Morris M. (2009). Diabetes and cardiovascular autonomic dysfunction: application of animal models. Auton. Neurosci. 145, 3-10.

Debono M. and Cachia E. (2007). The impact of Cardiovascular Autonomic Neuropathy in diabetes: is it associated with left ventricular dysfunction? Auton. Neurosci. 132, 1-7.

Dinçer U.D., Bidasee K.R., Güner S., Tay A., Ozçelikay A.T. and Altan V.M. (2001). The effect of diabetes on expression of beta1-, beta2-, and beta3-adrenoreceptors in rat hearts. Diabetes 50, 455-461.

Gando S., Hattori Y. and Kanno M. (1993). Altered cardiac adrenergic neurotransmission in streptozotocin-induced diabetic rats. Br. J. Pharmacol. 109, 1276-1281.

Giraldez R.R., Panda A., Xia Y., Sanders S.P. and Zweier J.L. (1997). Decreased nitric-oxide synthase activity causes impaired endothelium-dependent relaxation in the postischemic heart. J. Biol. Chem. 272, 21420-21426.

Goldstein D.S. (2003). Imaging of the autonomic nervous system: focus on cardiac sympathetic innervation. Semin. Neurol. 23, 423-433.

Haenen G.R., Veerman M. and Bast A. (1990). Reduction of beta-adrenoceptor function by oxidative stress in the heart. Free Radic. Biol. Med. 9, 279-288.

Huang M.T., Johnson E.F., Muller-Eberhard U., Koop D.R., Coon M.J. and Conney A.H. (1981). Specificity in the activation and inhibition

by flavonoids of benzo[a]pyrene hydroxylation by cytochrome P-450 isozymes from rabbit liver microsomes. J. Biol. Chem. 256, 10897-10901.

Ieda M. and Fukuda K. (2009). New aspects for the treatment of cardiac diseases based on the diversity of functional controls on cardiac muscles: the regulatory mechanisms of cardiac innervation and their critical roles in cardiac performance. J. Pharmacol. Sci. 109, 348-353.

Jeon T.J., Lee J.D., Ha J.W., Yang W.I. and Cho S.H. (2000). Evaluation of cardiac adrenergic neuronal damage in rats with doxorubicin-induced cardiomyopathy using iodine-131 MIBG autoradiography and PGP 9.5 immunohistochemistry. Eur. J. Nucl. Med. 27, 686-693.

Kim S.J., Lee J.D., Ryu Y.H., Jeon P., Shim Y.W., Yoo H.S., Park C.Y. and Lim S.G. (1996). Evaluation of cardiac sympathetic neuronal integrity in diabetic patients using iodine-123 metaiodobenzylguanidine. Eur. J. Nucl. Med. 23, 401-406.

Kiyono Y., Kajiyama S., Fujiwara H., Kanegawa N. and Saji H. (2005). Influence of the polyol pathway on norepinephrine transporter reduction in diabetic cardiac sympathetic nerves: implications for heterogeneous accumulation of MIBG. Eur. J. Nucl. Med. Mol. Imaging 32, 438-442.

Kusmic C., Morbelli S., Marini C., Matteucci M., Cappellini C., Pomposelli E., Marzullo P., L'abbate A. and Sambuceti G. (2008). Whole-body evaluation of MIBG tissue extraction in a mouse model of long-lasting type II diabetes and its relationship with norepinephrine transport protein concentration. J. Nucl. Med. 49, 1701-1706.

Liebgott T., Miollan M., Berchadsky Y., Drieu K., Culcasi M. and Pietri S. (2000). Complementary cardioprotective effects of flavonoid metabolites and terpenoid constituents of ginkgo biloba extract (EGb 761) during ischemia and reperfusion. Basic Res. Cardiol. 95, 368-377.

Lohse M.J., Engelhardt S. and Eschenhagen T. (2003). What is the role of beta-adrenergic signaling in heart failure? Circ. Res. 93, 896-906.

Maser R.E. and Lenhard M.J. (2005). Cardiovascular autonomic neuropathy due to diabetes mellitus: clinical manifestations, consequences, and treatment. J. Clin. Endocrinol. Metab. 90, 5896-5903.

Park A.M., Armin S., Azarbal A., Lai A., Chen P.S. and Fishbein M.C. (2002). Distribution of cardiac nerves in patients with diabetes mellitus: an immunohistochemical postmortem study of human hearts. Cardiovasc. Pathol. 11, 326-331.

Pietri S., Maurelli E., Drieu K. and Culcasi M. (1997). Cardioprotective and anti-oxidant effects of the terpenoid constituents of ginkgo biloba extract (EGb 761). J. Mol. Cell. Cardiol. 29, 733 - 742.

Rösen P., Ballhausen T., Bloch W. and Addicks K. (1995). Endothelial relaxation is disturbed by oxidative stress in the diabetic rat heart: influence of tocopherol as antioxidant. Diabetologia 38, 1157-1168.

Schmidt R.E., Beaudet L.N., Plurad S.B. and Dorsey D.A. (1997). Axonal cytoskeletal pathology in aged and diabetic human sympathetic autonomic ganglia. Brain. Res. 769, 375-383.

Schmidt R.E., Dorsey D.A., Beaudet L.N., Frederick K.E., Parvin C.A., Plurad S.B. and Levisetti M.G. (2003). Non-obese diabetic mice rapidly develop dramatic sympathetic neuritic dystrophy: a new experimental model of diabetic autonomic neuropathy. Am. J. Pathol. 163, 2077-2091.

Schneider R., Welt K., Aust W., Löster H. and Fitzl G. (2008). Cardiac ischemia and reperfusion in spontaneously diabetic rats with and without application of EGb 761: I. cardiomyocytes. Histol. Histopathol. 23, 807-817.

Schneider R., Welt K., Aust W., Löster H. and Fitzl G. (2009). Cardiac ischemia and reperfusion in spontaneously diabetic rats with and without application of EGb 761: II. Interstitium and microvasculature. Histol. Histopathol. 24, 587-598.

Sethi R., Shao Q., Takeda N. and Dhalla N.S. (2003). Attenuation of changes in G(i)-proteins and adenylyl cyclase in heart failure by an ACE inhibitor, imidapril. J. Cell. Mol. Med. 7, 277-286.

Scott L.A. and Kench P.L. (2004). Cardiac autonomic neuropathy in the diabetic patient: does 123I-MIBG imaging have a role to play in early diagnosis? J. Nucl. Med. Technol. 32, 66-71.

Sharma V. and McNeill J.H. (2006). Diabetic cardiomyopathy: where are we 40 years later? Can. J. Cardiol. 22, 305-308.

Sharma V., Parsons H., Allard M.F. and McNeill J.H. (2008). Metoprolol increases the expression of beta(3)-adrenoceptors in the diabetic heart: effects on nitric oxide signaling and forkhead transcription factor-3. Eur. J. Pharmacol. 595, 44-51.

Standl E. and Schnell O. (2000). A new look at the heart in diabetes mellitus: from ailing to failing. Diabetologia 43, 1455-1469.

Taniguchi N., Arai K. and Kinoshita N. (1989). Glycation of copper/zinc superoxide dismutase and its inactivation: identification of glycated sites. Methods Enzymol. 179, 570-581.

Togane Y. (1999). Evaluation of the cardiac autonomic nervous system in spontaneously non-insulin-dependent diabetic rats by 123I-metaiodobenzylguanidine imaging. Ann. Nucl. Med. 13, 19-26.

Verberne H.J., Brewster L.M., Somsen G.A. and van Eck-Smit B.L. (2008). Prognostic value of myocardial 123I-metaiodobenzylguanidine (MIBG) parameters in patients with heart failure: a systematic review. Eur. Heart J. 29, 1147-1159.

Vinik A.I. and Ziegler D. (2007). Diabetic cardiovascular autonomic neuropathy. Circulation 115, 387-397.

Vinik A.I., Maser R.E., Mitchell B.D. and Freeman R. (2003). Diabetic autonomic neuropathy. Diabetes Care 26, 1553-1579.

Yagihashi S. (1995). Pathology and pathogenetic mechanisms of diabetic neuropathy. Diabetes Metab. Rev. 11, 193-225.

Yagihashi S. and Sima A.A. (1985). Diabetic autonomic neuropathy. The distribution of structural changes in sympathetic nerves of the BB rat. Am. J. Pathol. 121, 138-147.

Yagihashi S. and Sima A.A. (1986). Diabetic autonomic neuropathy in BB rat. Ultrastructural and morphometric changes in parasympathetic nerves. Diabetes 35, 733-743.

Yagihashi S., Zhang W.X. and Sima A.A. (1989). Neuroaxonal dystrophy in distal symmetric sensory polyneuropathy of the diabetic BB-rat. J. Diabet. Complications 3, 202-210.

Zhang X.M., Shen F., Xv Z.Y., Yan Z.Y. and Han S. (2005). Expression changes of thrombospondin-1 and neuropeptide Y in myocardium of STZ-induced rats. Int. J. Cardiol. 105, 192-197.

Zhu W.Z., Wang S.Q., Chakir K., Yang D., Zhang T., Brown J.H., Devic E., Kobilka B.K., Cheng H. and Xiao R.P. (2003). Linkage of beta1-adrenergic stimulation to apoptotic heart cell death through protein kinase A-independent activation of Ca2+/calmodulin kinase II. J. Clin. Invest. 111, 617-625.

Accepted June 16, 2010